

## Determination of the relative soil compactness in the foundation condition by microgravity data

V.E. ARDESTANI

*Inst. Geophysics, University of Teheran and Center of Excellency in Survey Eng. and Disaster Manag., Tehran, Iran*

(Received: September 26, 2011; accepted: February 4, 2013)

**ABSTRACT** Low-density zones with high void ratio can be detected in the foundation condition by microgravity data. After collecting the data and using standard corrections methods, Bouguer anomalies are computed. Residual anomalies are obtained by removing the trend or regional anomalies from Bouguer anomalies. Negative anomalies are quite distinguishable in residual anomalies map. One of the most important causes of low-density zones is the decrease of soil compactness due to the high void ratio. These detected low-density or low-compacted zones should be grouted before any kind of construction. These zones are associated with lows in microgravity data and relative negative anomalies consequently. These detected negative anomalies seem to be interconnected in some way. This connection advocates the hypothesis of a common source for these anomalies. The detected low-compacted zones are examined and confirmed by a few number of test pits. One of the pits encountered an underground man-made water supply. Some other test pits encountered loose or low-compacted zones that were filled with water after a few hour of drilling, originated from the detected man made water supply.

**Key words:** Soil compactness, microgravity data, foundation condition.

### 1. Introduction

The difference in the densities of subsurface materials is the basic concept of microgravity surveys. Microgravity is an effective method to detect areas (zones) of contrasting or anomalous density by measuring the variation of the gravity acceleration of the Earth. One of the main source of local lows in microgravity data are the low density zones in the shallow subsurface. These zones are characterized by compactness or high void ratio in soil mechanical experiment.

Several examples of successful microgravity surveys have been described in the past over large features including natural cavities (Patterson *et al.*, 1995; Cooper, 1998; Styles *et al.*, 2005; Ardestani, 2008). The object of these papers and many others published concerns cavity detection in the rocks. A few examples of microgravity surveys concern the application of the method in soils and estimating the soil mechanic parameters such as compactness or void ratio. Tuckwell *et al.* (2008) detected the small distributed voids and low-density zones by microgravity that were subsequently proved by dynamic probing.

## 2. Site character and geology

The site under investigation is located in a semi-urban area close to Mohammad-Shahr where a market is under construction.

The site is formed by horizontal layers of alluvium with high compactness and well graded materials [see the geotechnical report in: Sad-Azma Tiva Company, (2010)].

After removing the residual soil to the depth of 5 m, a few collapses happened at the surface ground of the foundation over night (Figs. 1 and 2) in spite of good geotechnical results on well compactness. On the other hand, the collapsed pits show a specific orientation which advocate the existence of some buried subsurface voids and cavities. Moreover, an old demolished factory is very close to the site and so there may be several natural or man-made underground water supply or waste water channels originated from the factory and passing across the site.

## 3. Soil compactness

Compactness is one of the most important parameters in classifying the strength and type of the soils according to soil mechanic engineering point of view. The soils with low compactness could be susceptible to collapse under the influence of additional load from building foundations, etc.

This parameter is defined through the definition of relative compactness (Memarian, 2008):

$$Dr = \frac{1/\delta l - 1/\delta n}{1/\delta l - 1/\delta d} \quad (1)$$

where  $\delta n$  is the natural density,  $\delta d$  is the maximum density,  $\delta l$  is the density in loose condition and  $Dr$  is the relative compactness.

Based on the relative compactness, the soils are classified from very loose to very compact. The densities in Eq. (1) can be determined by sampling the soils and by standard tests in laboratory, for instance, Standard Proctor Test (Memarian, 2008). Some other tests can be done in situ such as, Dynamic Probing Test, Standard Penetrating Test (SPT) and Cone Penetrating Test (CPT). It is worth to mention that all these tests are carried out in a few samples or bore holes and so the obtained results are not representative for the whole parts of the site particularly in the areas that where natural or man-made voids may exist.

### 3.1. Soil compactness in the survey area

To estimate the compactness, SPT tests have been performed in 4 boreholes and the results are shown in Figs. 3 to 6. Inspecting these figures, we observe that the SPT values are higher than 60 or 70 at depth higher than 1.5 - 2.5 m from ground surface.

These values of SPT represent a compact to very compact soil. Therefore, the reason of the collapses should be based on secondary sources such as an increase of the void ratio due to the leakage of the water from probable water or waste water underground wells or tunnels. This leakage has been proved by the rapid disappearance of grouted water in one of the collapsed pits.



Fig. 1 - Foundation and collapsed pit.



Fig. 2 - Foundation and collapsed pit.

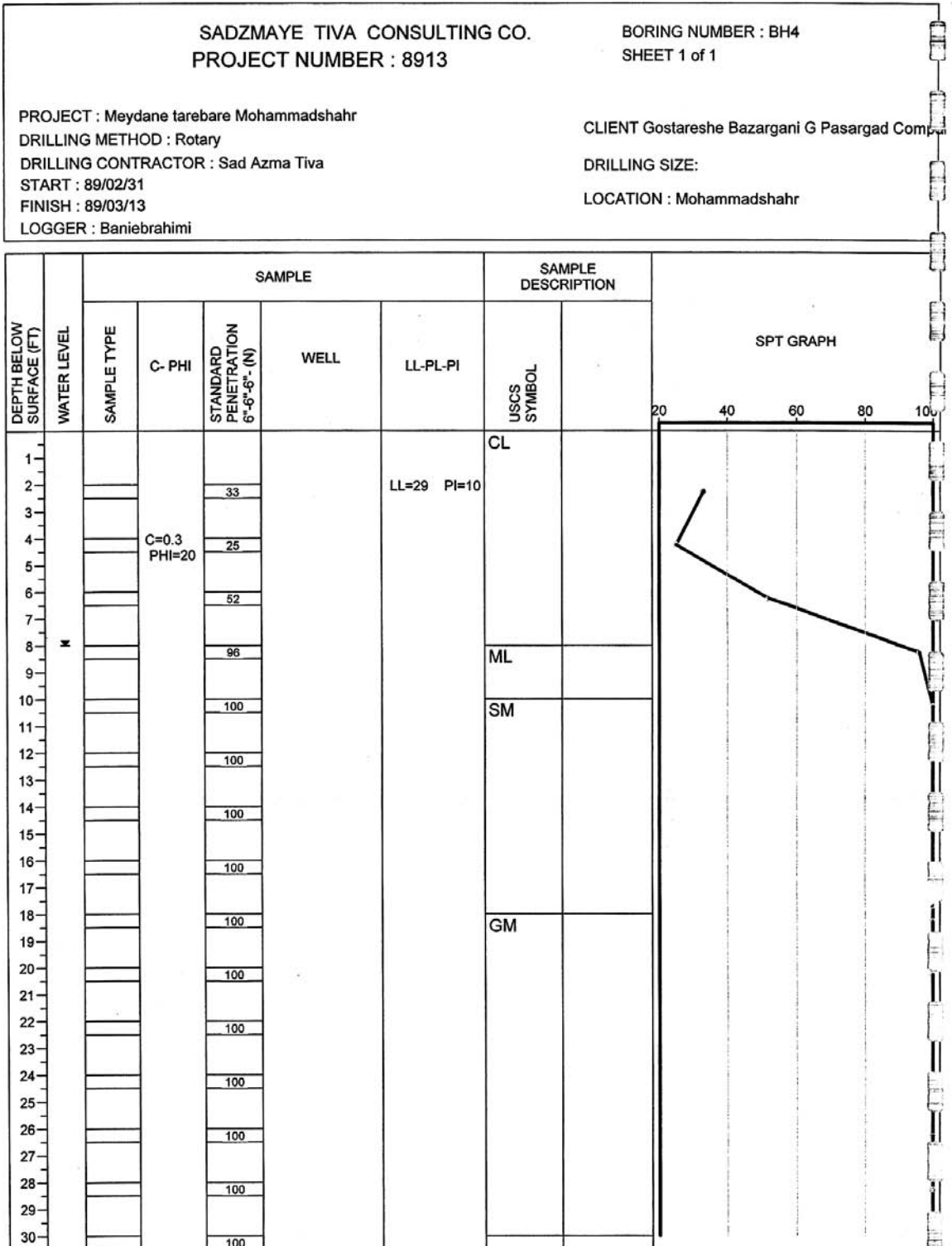


Fig. 3 - Geotechnical borehole.

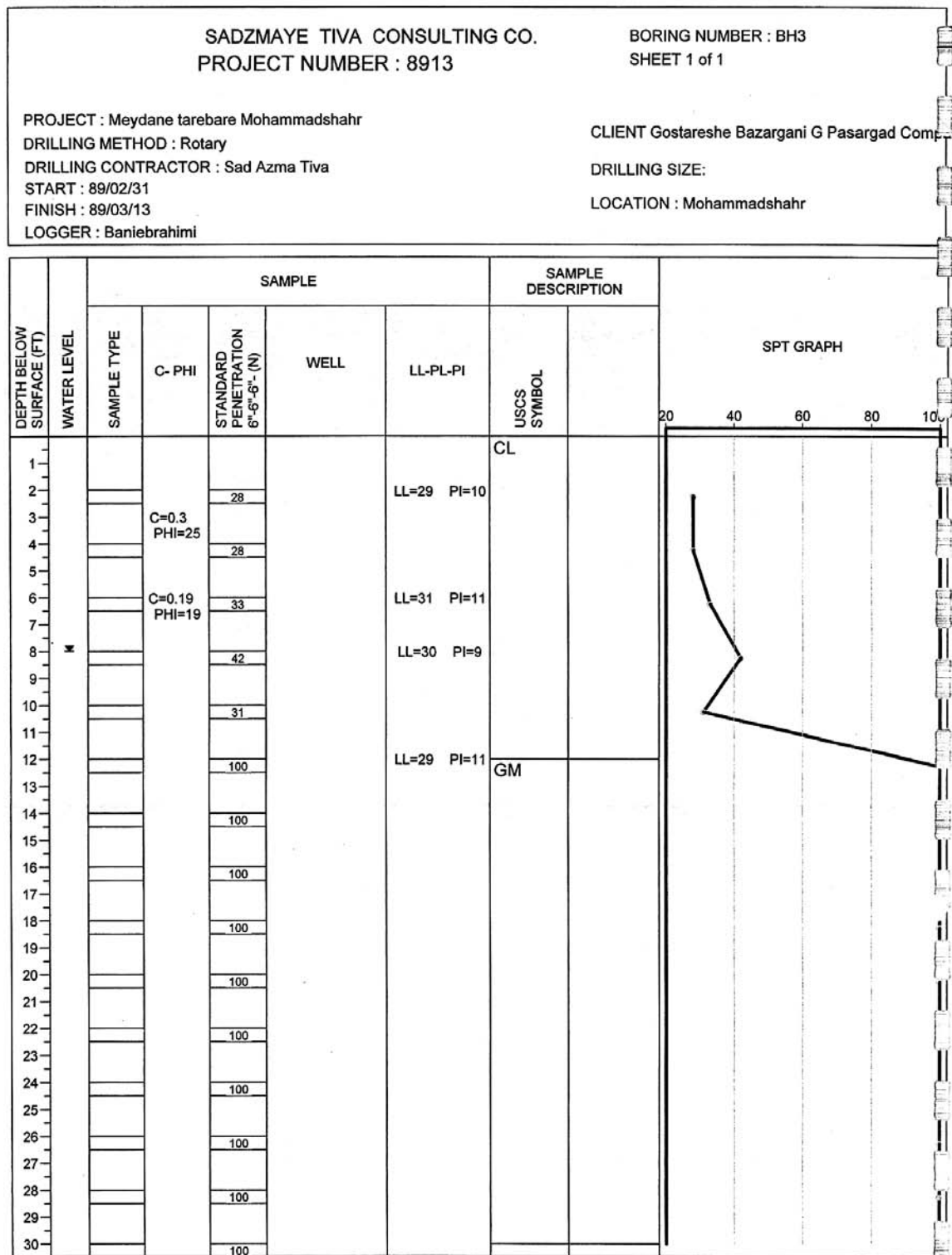


Fig. 4 - Geotechnical borehole.

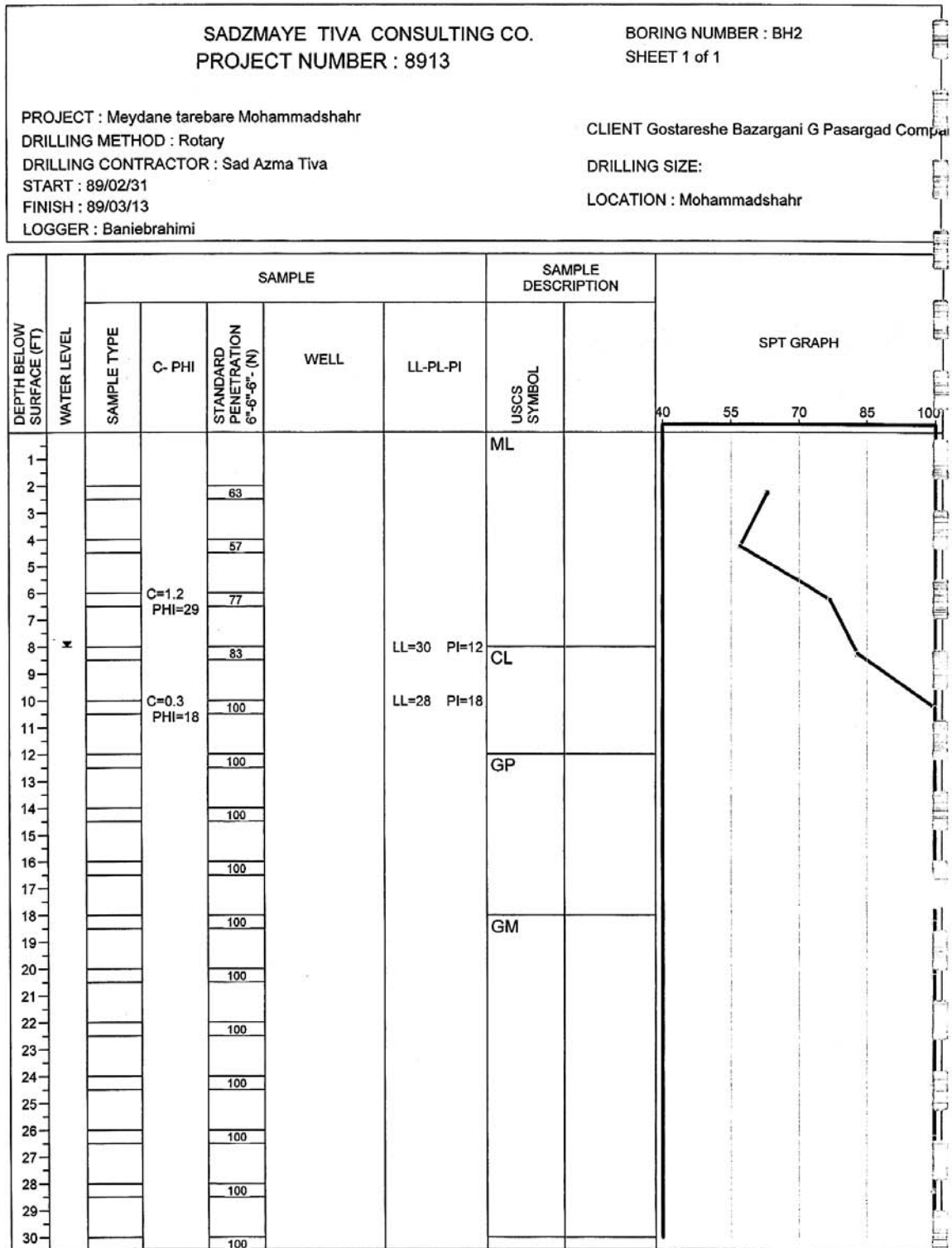


Fig. 5 - Geotechnical borehole.

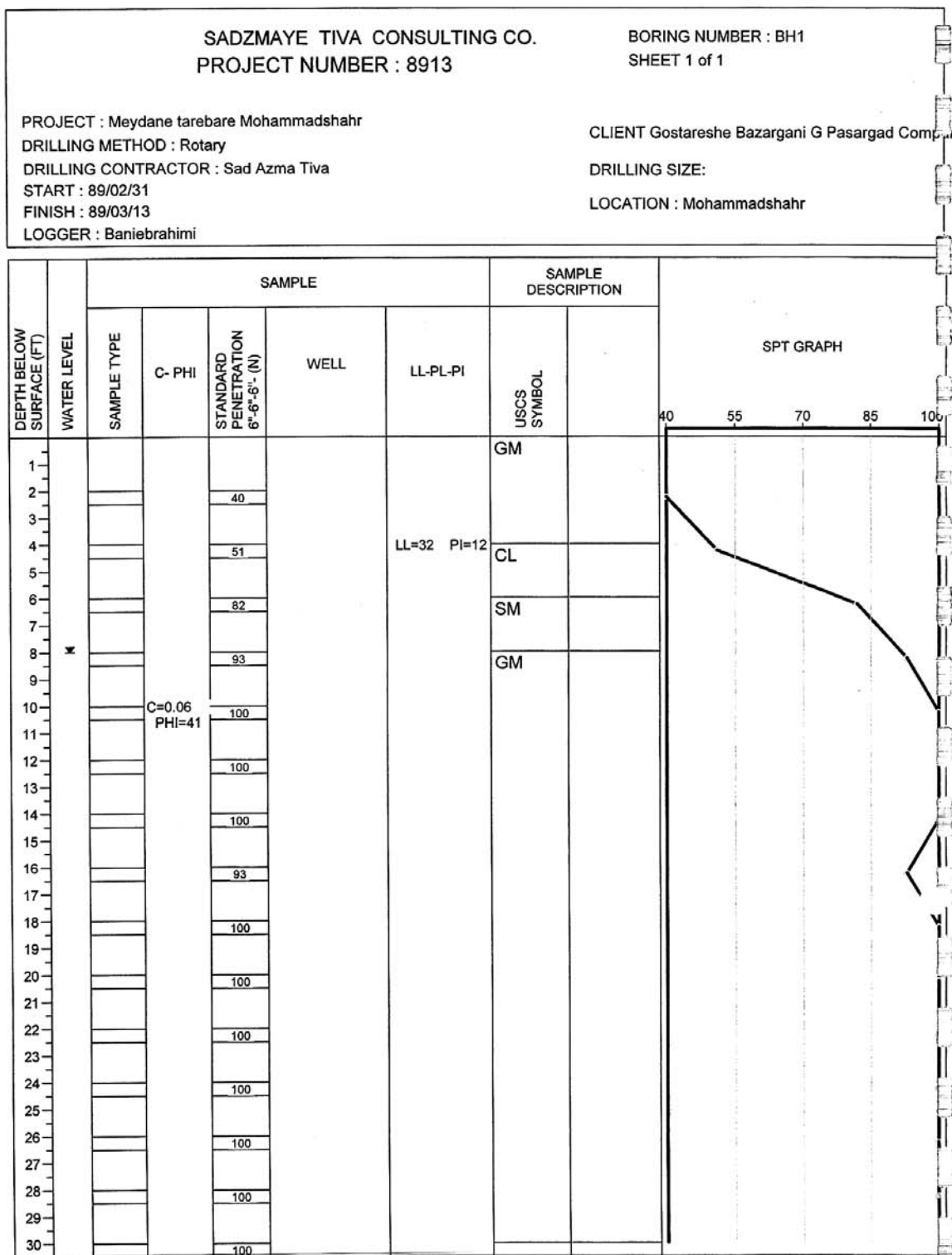


Fig. 6 - Geotechnical borehole.

#### 4. Field procedure of microgravity survey

The microgravity grid consists of 1000 measurement points over an area with dimension of about 40 by 100 m. A basic grid dimension of 2 m is used. Data were collected with a CG3-M gravimeter with a sensitivity of approximately 1  $\mu\text{Gal}$ . The coordinates of the points have been measured by a RTK dual frequency GPS (Trimble R7, R8) with an accuracy less than 1 cm in positioning and about 2 mm in elevation.

#### 5. Gravity corrections

A base point has been selected in the area and all the measurements have been referenced to this point. The long-term drift of gravimeter has been removed by continuous reading (cycling mode) at the Institute of Geophysics. To remove the short-term drift, the measurements were repeated at the base point at each hour of the work day and the maximum drift was equal to 5  $\mu\text{Gal}$ . The Bouguer density has been obtained from the geotechnical report (Sad-Azma Tiva Company, 2010) and is equal to 2000  $\text{kg/m}^3$ . To compute Bouguer anomalies, a standard approach has been followed.

The first correction is latitude correction that is carried out by using the following equation:

$$g_l = 0.000812132(\sin 2l) y_s \quad (2)$$

where  $l$  is latitude of station and  $y_s$  is the station distance north of the grid origin in metre.

The free-air correction has been computed by the following standard formula:

$$\delta g_f = \pm 0.3086h \quad (3)$$

where  $h$  is the relative elevation of the measuring points.

The Bouguer correction has been computed by the following formula:

$$\delta g_B = \pm 2\pi G \rho h \quad (4)$$

where  $G$  is the universal gravitational constant and  $\rho$  is the Bouguer density.

In this survey the terrain corrections are actually the gravity effects of the surrounding buildings. There are not so tall buildings up to a radius of 200 m from the site and so the terrain effect is only considered for the influence of the buildings beyond this distance. The gravity effects of the buildings can be computed through the following equation of the gravity effect of rectangular prism (Nagy, 1966):

$$g = -G\rho \left[ \left| \frac{z_2}{z_1} \right| \left| \frac{y_2}{y_1} \right| \left| \frac{x_2}{x_1} \right| x \ln(y+R) + y \ln(x+R) + Z \operatorname{tg}^{-1} \left( \frac{Z.R}{x.y} \right) \right] \quad (5)$$

where  $G$  is the gravitational constant,  $\rho$  the density and  $x_1, y_1, z_1$  and  $x_2, y_2, z_2$  are the Cartesian



coordinates of the left lowermost and right uppermost corners of the prism in a right angle coordinate system respectively and:

$$R = \sqrt{x^2 + y^2 + z^2}. \quad (6)$$

The Bouguer gravity anomalies have been computed by means of Eqs. (2), (3) and (4) as follows:

$$gB = (gobs \pm \delta gf \pm \delta gB) - gbase \quad (7)$$

where *gbase* is the reference gravity value at the base point.

## 6. Error analysis and precision requirements

As the sources of microgravity anomalies are shallow minor geological structures close to the ground surface, their effects are commonly between 10 - 100  $\mu$ Gal. So that the resolving capability of gravity anomaly should be limited within the range of 5 - 10  $\mu$ Gal and the observation error should never exceed 5  $\mu$ Gal. This accuracy is attainable considering the maximum drift equal to 5  $\mu$ Gal in this survey. As the effect of some environmental source of errors such as temperature, variation of magnetic field, variation of atmospheric pressure are diminished substantially in CG3 gravimeter, we could keep the observation error in less than 5  $\mu$ Gal or better to say 10 $\mu$ Gal with reading the base point once per hour repeatedly.

Error of positioning is required to be less than 1 m so as to ensure the latitude correction to be less than 1  $\mu$ Gal which is quite satisfied in this survey.

An error of  $\pm 0.3$  cm of relative elevation would cause the error of free-air correction to be less than 1  $\mu$ Gal for a given density. The error due to relative elevation in Bouguer correction is far less than in free-air correction. So the accuracy in relative elevation should not exceed 0.3 cm or 3 mm that is relatively satisfied by our leveling system.

If the accuracy of the estimated Bouguer density is within 20  $\text{kg/m}^3$ , the error of Bouguer correction would be less than  $\pm 1$   $\mu$ Gal. As the density is estimated through geotechnical on site measurements, it can be accurate and reliable in this survey.

So if the density is determined with an error less than  $\pm 20$   $\text{kg/m}^3$  and an error less than  $\pm 0.3$  cm in relative elevation determination, the error of Bouguer correction [Eq. (3)] should be  $\pm 1$   $\mu$ Gal or even less. The eventual error of Bouguer anomaly calculated as based upon the previous errors may be less than  $\pm 6$   $\mu$ Gal.

In the case of terrain correction that are the gravity effects of surrounding buildings, the diagrams presented by Qianshen *et al.* (1996) have been used. These diagrams determine the minimum influential distance that the gravity effect of located buildings should be considered as the terrain effects in this distance. In other words, the diagrams determine the distance of terrain correction.

In this survey this distance is about 250 m by considering the dimensions of the buildings and if the maximum error is allowed to be 1  $\mu$ Gal.

As we do not have any building up to 200 m distance, the effects of the building between 200

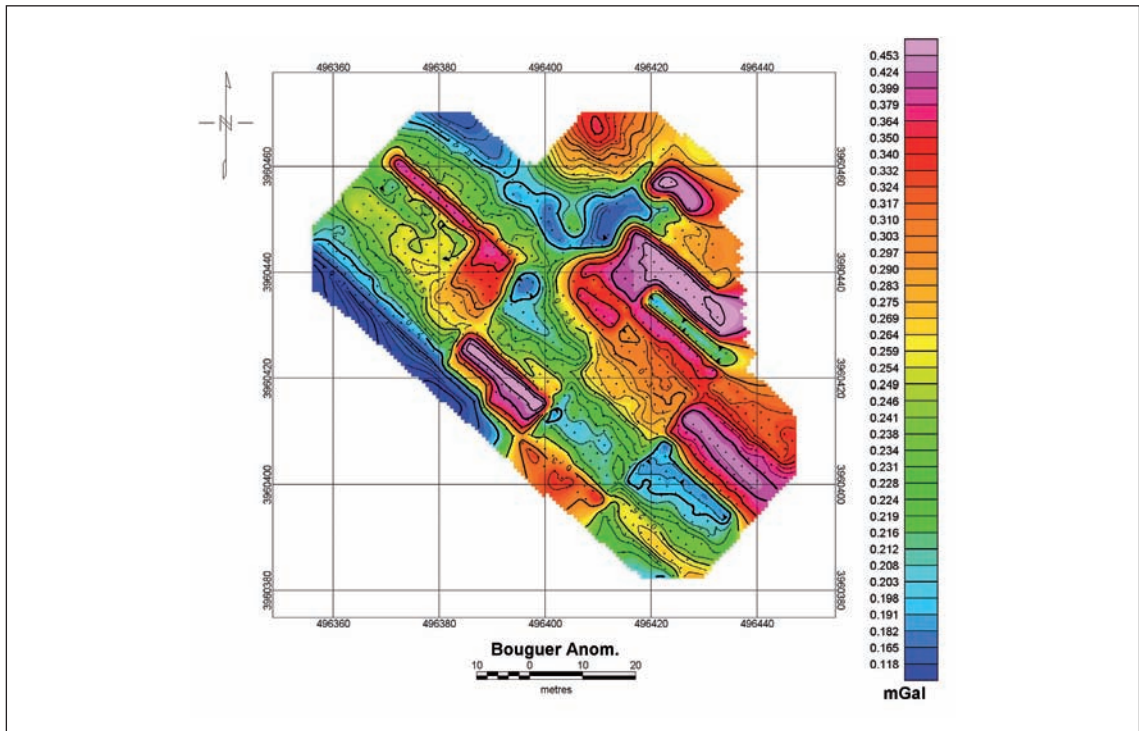


Fig. 7 - Bouguer anomalies (mGal).

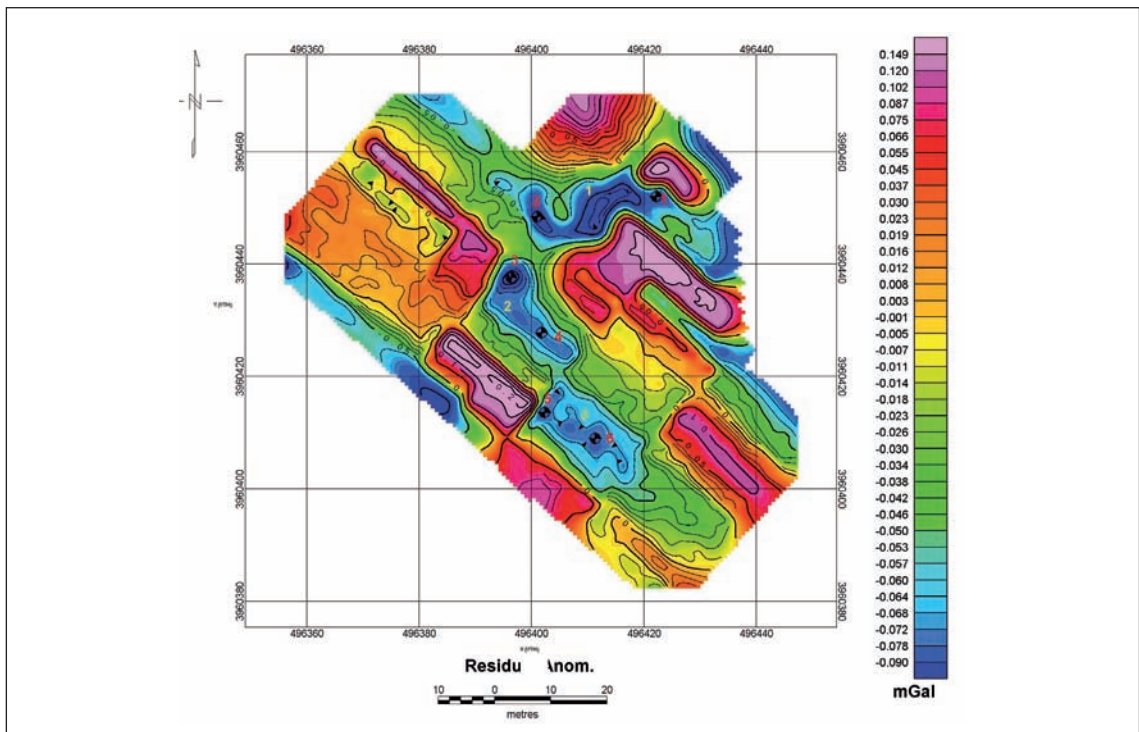


Fig. 8 - Residual anomalies (mGal).

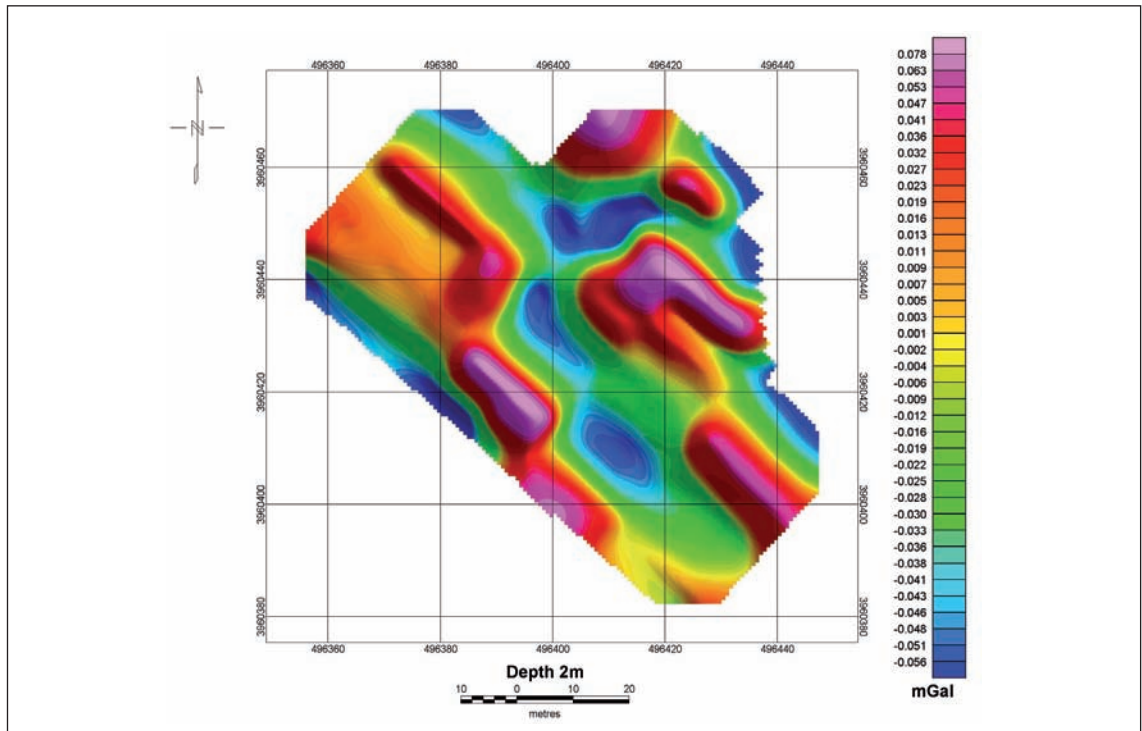


Fig. 9 - Upward continuation (2 m).

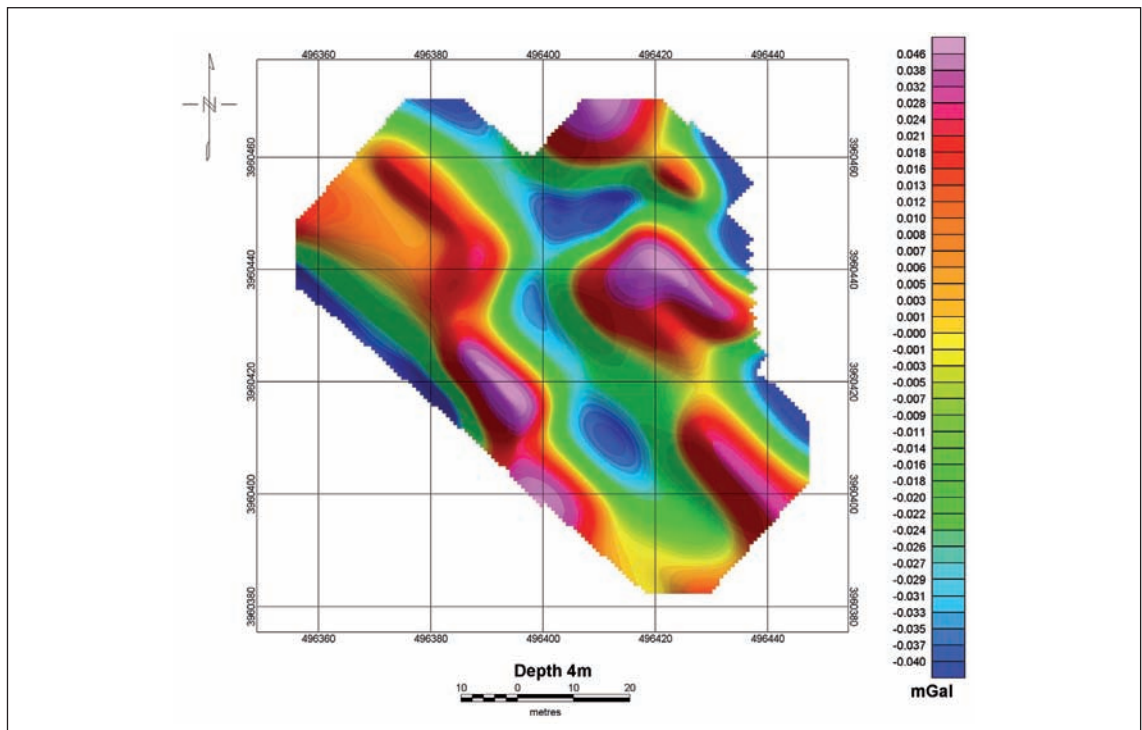


Fig. 10 - Upward continuation (4 m).

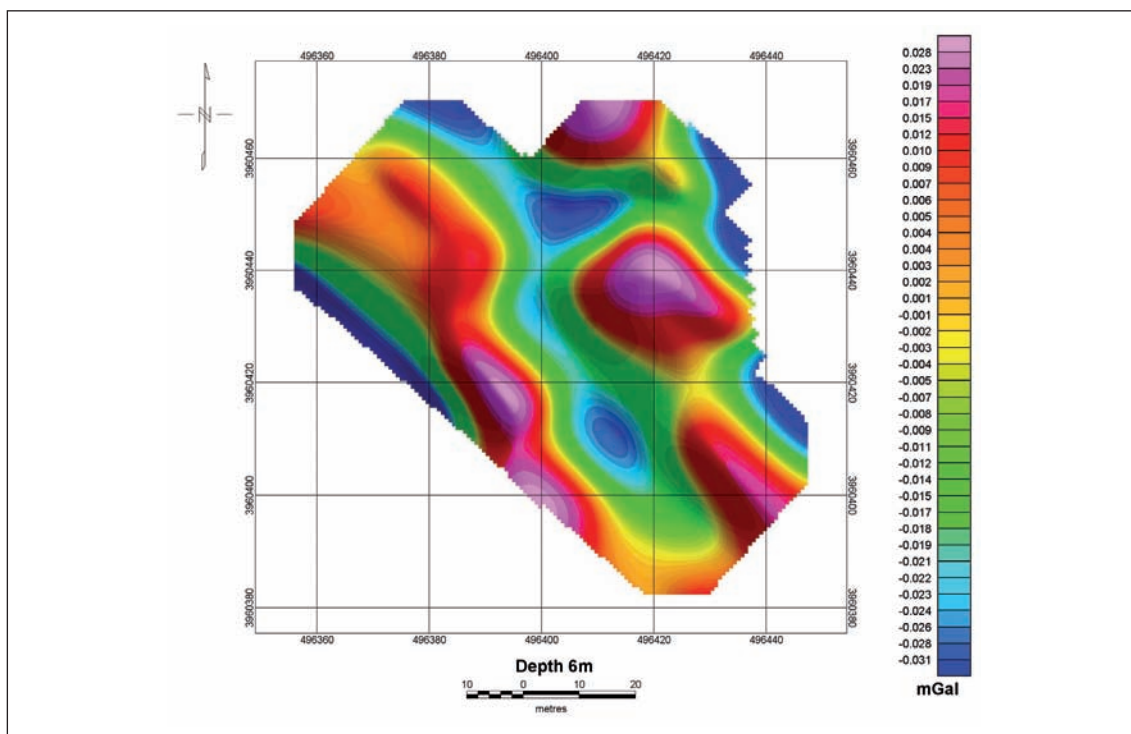


Fig. 11 - Upward continuation (6 m).

to 250 m radius should only be considered. The maximum gravity effect of these buildings that are mostly residential houses is about 3  $\mu$ Gal as computed through Eq. (4). Hence, the gravity effects of the building can be accurately estimated although being such effects very minor in this survey.

### 7. Data processing

After gravity corrections, the computed Bouguer anomalies are shown in Fig. 7. The relative negative anomalies, caused by probable voids or low-density ground in general, are represented by dark blue color in this figure. The main negative anomalies are located at the place of the collapsed pits at the centre of the grid and expanded as a channel toward east.

Several other negative anomalies are also distinguishable which seem to be branched from the main channel of negative anomalies.

Residual anomalies have been computed using the polynomial fitting method to highlight local anomalies and the results are shown in Fig. 8.

We used the following equations to compute the polynomials:

$$g(x, y) = \sum_{q=0}^t \sum_{p=0}^s V_{pq} x_i^p y_i^q \tag{8}$$

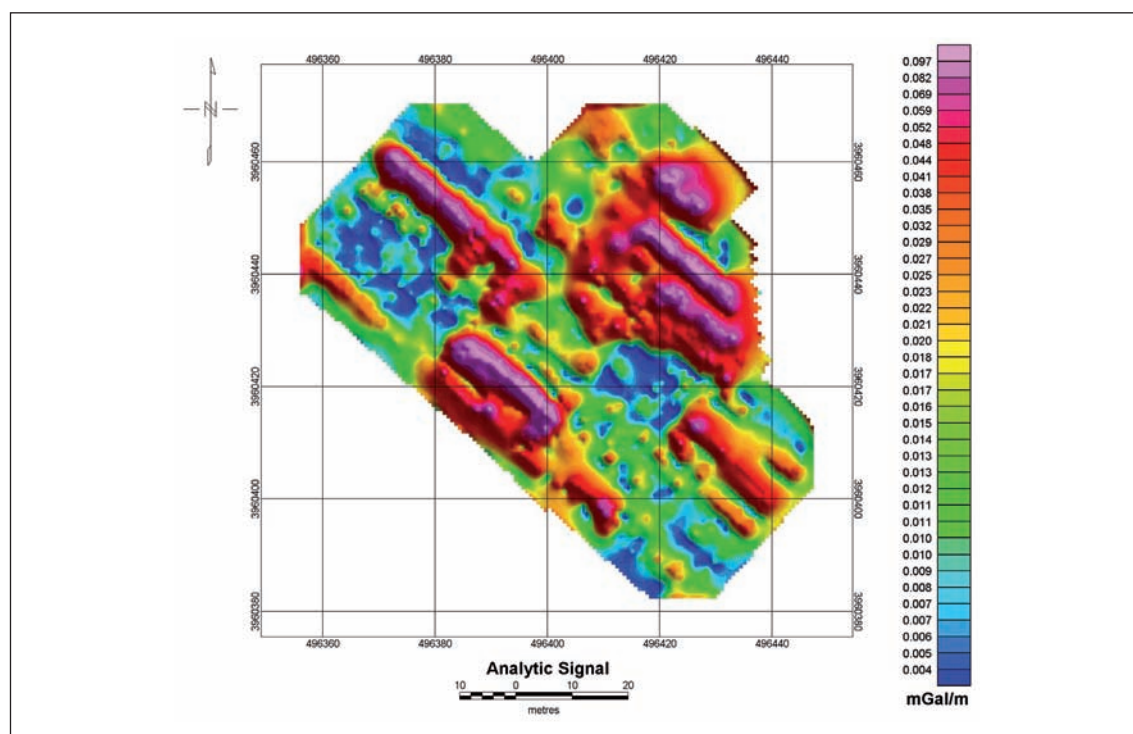


Fig. 12 - Analytic signal (mGal/m).

where  $q$  is the degree and  $V$  represent the indexes of the polynomial which have to be computed through least-square method and  $x$  and  $y$  are the coordinates of the gravity points.  $g(x,y)$  is the regional gravity anomaly that is subtracted from the Bouguer anomalies to compute the residual anomalies at each point. The determination of the proper degree is quite important. The more complex the Bouguer anomalies map the higher the degree. Usually the degrees 2 or 3 are suitable but anyway the proper degree is subject to interpreter. Using Eq. (7) three main zones of negative anomalies are numbered in Fig. 8. It seems that these anomalies are somehow connected.

In order to estimate the maximum depth of these anomalies, the principle by Jacobson (1987) has been used and the results are shown in Figs. 9 to 11. In this principle, half distance of upward continuation is considered as the depth of the downward continuation. The distance at which the effects of the anomalies disappear will be considered as the maximum depth. The upward continuation has been computed using Fourier transform (Jacobson, 1987). From Figs. 9 to 11, the maximum depth of these negative anomalies are in the range 4 to 6 m.

For edge detection of the anomalies, the analytic signal method is applied and the results are shown in Fig. 12. The amplitude of analytic signal can be calculated through the following equation:

$$As = \sqrt{(\partial g / \partial x)^2 + (\partial g / \partial y)^2 + (\partial g / \partial z)^2} \quad (9)$$

where  $g$  is the residual anomalies and the maximum of  $As$  which represents the analytic signal amplitude, locates on the edges of the anomalies.

## 8. Drilling results and discussion

Before the microgravity survey, a great quantity of water has been grouted in one of the collapsed pits (Fig. 2) which is located at the peak of the negative anomaly number 2 (Fig. 8). The water disappeared in a few hours.

In order to investigate the results of the microgravity survey, several test pits have been proposed (Fig. 8). Four of these test pits (numbers 1, 4, 5 and 6) have been drilled and pits numbers 2 and 3 are located inside the collapsed pit (Figs. 1 and 2).

Pit number 1 encountered a man made underground water supply at depth of about 2 m which extended to the east and at the location of the peak of the negative anomaly number 1 (Fig. 8).

Pits number 4, 5 and 6 encountered a loose soil at depth of about 4 to 5 m and were filled by water in a few hours. As the depths of the base of these test pits are much higher than the water table in the area, the only hypothesis for the water gathered in them is the leakage of the supplied water at the location of anomaly number 1 to this area.

In other words, this supplied water caused the observed collapses and penetrated into the pits number 4, 5 and 6.

Therefore the negative zones numbered 1, 2 and 3 are connected to each other by continuous subsurface voids or hydro-geological channels.

On the other hand, the analytic signal map (Fig. 12) does not show maximum values at the location of anomalies number 2 and 3. So the hypothesis of existing man-made channel is not proved and the only explanation is high void ratio and consequently high porosity and low compactness.

## 9. Conclusion

Microgravity is a valuable method to detect voids and low-density ground in general. The method can be applied before geotechnical experiments to determine the critical zones for sampling or for in situ soil mechanic tests and is actually a guide map for the proper location of the tests. Otherwise, the results of geotechnical tests could either be wrong or not representative of the characteristics of the entire survey area.

**Acknowledgements.** The author is very thankful to the authorities of the Anbohsazan Pasargad company and particularly to Mr. Khorram for sponsoring the project and from Sad-Azma company for providing us with the geotechnical report. I am also thankful to the authorities of the Institute of Geophysics, University of Tehran for all supports. Special thanks should be devoted to Mr. Salimi for measuring the field data.

## REFERENCES

- Ardestani V.E.; 2008: *Modelling the Karst zones in a dam site through micro-gravity data*. Explor. Geophys., **39**, 204-209.
- Cooper A.H.; 1998: *Subsidence hazards caused by the dissolution of Permian gypsum in England: geology, investigation and remediation*. In Maund J.G. and Eddleston M. (eds), *Geohazards in Engineering Geology*, Geological Society, London, Engineering Special Publications, Vol. 15, pp. 265-275.
- Jacobson H.; 1987: *A case for upward continuation as a standard separation filter for potential field maps*. Geophys., **52**, 1138-1145.
- Memarian H.; 2008: *Engineering geology and geotechnics*. University of Tehran, Iran, 953 pp. (in Persian).
- Nagy D.; 1966: *The gravitational attraction of a right rectangular prism*. Geophys., **31**, 362-371.
- Patterson D.A., Davey J.C., Cooper A.H. and Ferris J.K.; 1995: *The investigation of dissolution subsidence incorporating microgravity geophysics at Ripon*. Q. J. Eng. Geol. Hydrogeol., **28**, 83-94.
- Qianshen W., Chijum Z., Fuzhen J. and Wenhui Z.; 1996: *Microgravimetry*. Science Press, Beijing, China, 146 pp.
- Sad-Azma Tiva Company; 2010: Geotechnical report of Mohammad Shahr site.
- Styles P., McGrath R., Thomas E. and Cassidy N.J.; 2005: *The use of microgravity for cavity characterization in karstic terrains*. Q. J. Eng. Geol. Hydrogeol., **38**, 155-169.
- Tuckwell G., Grossey T., Owen S. and Stearns P.; 2008: *The use of microgravity to detect small distributed voids and low-density ground*. Q. J. Eng. Geol. Hydrogeol., **41**, 371-380.

Corresponding author: Vahid E. Ardestani  
Institute of Geophysics, University of Tehran, Iran  
Center of Excellency in survey engineering and disaster management  
Kargar Shomali St., P.O. Box 14155-6466, Tehran, Iran  
Phone: 0098 21 61118232; fax: 0098 21 88630548; e-mail: ebrahimz@ut.ac.ir

